

Unbalanced Homodyne Correlation Measurements

B. Kühn and W. Vogel

Arbeitsgruppe Quantenoptik, Institut für Physik, Universität Rostock, D-18051 Rostock, Germany

(Dated: June 12, 2022)

A method is introduced which allows to measure normal-ordered moments of the displaced photon-number operator up to high orders. It is based on unbalanced homodyne correlation measurements, the local oscillator being replaced by a displaced dephased laser. The measured moments yield a simple approximation of the full quantum state, which is obtained without the need of photon-number resolution. Quantum properties of light are efficiently certified through the direct detection of normal-ordered observables, which is illustrated for a weakly squeezed vacuum and a single-photon-added thermal state.

PACS numbers: 42.50.Dv, 03.65.Ta, 42.50.Lc, 03.65.Wj

I. INTRODUCTION

Phase-sensitive measurements of light play a key role for any application of radiation fields, both in classical and quantum physics, or technology. For this purpose, homodyne measurement techniques were introduced [1]. They rely on the superposition of the signal with a coherent reference field – the local oscillator (LO). Excess noise of the usually strong LO can be eliminated via balanced homodyne detection [2, 3]. In quantum optics this opened the possibility to fully characterize quantum states of light [4–7], for reviews see [8–10]. Unbalanced homodyne detection with a weak LO yields a simple determination of the quantum state [11, 12]. As it needs to distinguish adjacent photon numbers, it could be realized for extremely weak signals only [13].

Another important development was the application of correlation measurement techniques, for the experimental demonstration of the quantum nature of light through the antibunching of photons in atomic resonance fluorescence [14]. A strong point is that the measured intensity correlations are normal and time ordered, and hence insensitive to vacuum-noise effects. For the measurement of phase-sensitive squeezing in atomic resonance fluorescence, small quantum efficiencies in homodyne detection pose a severe problem [15]. To overcome this deficiency, homodyne correlation measurements with a weak LO were proposed [16, 17]. Only very recently this technique has been applied to detect squeezing in resonance fluorescence from a semiconductor quantum dot [18], see also [19–21] for related techniques. These methods were further developed to combine the advantages of homodyne correlation and balanced measurements [22]. Using a strong LO, normal-ordered quadrature moments of high orders are accessible by this balanced homodyne correlation technique.

In this contribution we introduce an unbalanced homodyne correlation measurement (UHCM) technique. The aim is to unify the simplicity of quantum state characterization by unbalanced homodyne detection with the loss insensitivity of homodyne correlation measurements. For this purpose, the LO is replaced by a coherently displaced dephased laser (DDL). The dephasing is needed

to detect normal-ordered photon-number moments up to high orders by eliminating the coherences of quadrature moments. The displacement eventually yields normal-ordered moments of the displaced photon number operator. The strong point of the method is that both photon-number resolving detectors and complex balancing of the setup become superfluous. We apply our method to verify nonclassical phenomena of light by properly constructed and directly accessible nonclassicality witnesses.

II. MEASUREMENT TECHNIQUE

The state of single mode light can be fully represented by the s -parametrized quasiprobabilities of Cahill and Glauber [23], which can be given in the simple form [12]

$$P(\alpha; s) = \frac{2}{\pi(1-s)} \sum_{k=0}^{\infty} \left[\frac{\eta(1-s) - 2}{\eta(1-s)} \right]^k p_k(\alpha), \quad (1)$$

with s being the ordering parameter and η the quantum efficiency. It depends on the photoelectric counting statistics $p_k(\alpha)$ of the coherently displaced quantum state, $\hat{\rho} \mapsto \hat{\rho}(-\alpha)$,

$$p_k(\alpha) = \left\langle : \frac{(\eta \hat{n}(\alpha))^k}{k!} e^{-\eta \hat{n}(\alpha)} : \right\rangle. \quad (2)$$

Here $\hat{n}(\alpha) = (\hat{a}^\dagger - \alpha^*)(\hat{a} - \alpha)$ is the displaced photon number operator. The symbol $: \cdot :$ denotes normal ordering of the annihilation and creation operators \hat{a} and \hat{a}^\dagger , respectively. Even in the case of imperfect detection, for quantum efficiencies $\eta < 1$, the quantum state is obtained through Eq. (1) from the measured statistics.

The unbalanced homodyne detection method for the experimental state reconstruction is based on the measurement of the displaced photon-number statistics (2). Approaches were introduced in Ref. [11] for the Wigner function, in Ref. [12] for general s -parametrized quasiprobabilities, and in Ref. [24] for more general regular quasiprobabilities. In principle, the experimental implementation of these state reconstructions requires photon-number resolving detectors. The accessible photon numbers are typically very small [13], so that a truncation of the photon number in Eq. (1) is indispensable.

This necessitates preknowledge on the state under study and involved studies of systematic errors [24].

Obviously, the statistics (2) is related to normal-ordered displaced photon number moments,

$$p_k(\alpha) = \sum_{\ell=k}^{\infty} (-1)^{\ell-k} \frac{\eta^\ell}{(\ell-k)! k!} \langle : [\hat{n}(\alpha)]^\ell : \rangle. \quad (3)$$

Therefore, the knowledge of all these moments fully determines the quantum state as well. Our UHCM technique will render it possible to measure the moments $\langle : [\hat{n}(\alpha)]^m : \rangle$ with linear standard detectors.

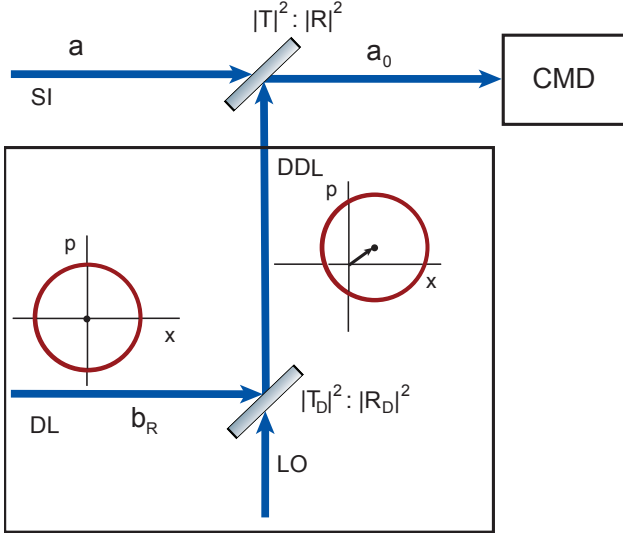


FIG. 1. (Color online) Experimental UHCM setup. The signal (SI) is combined with a displaced dephased laser (DDL) at a highly transmissive beam splitter. The output \hat{a}_0 is recorded via a correlation measurement device (CMD), which yields the moments $\langle : [\hat{n}(\alpha)]^m : \rangle$.

The basic setup of our measurement technique is illustrated in Fig. 1. The signal \hat{a} is combined with the displaced dephased laser (DDL) by a beam splitter of high transmissivity, with amplitude transmittance and reflectance T and R , respectively. The DDL replaces the local oscillator used in standard homodyne detection. This unusual reference field is used to accomplish that the moments $\langle : [\hat{n}(\alpha)]^m : \rangle$ are directly extracted from the detection of the output field \hat{a}_0 of the beam splitter with a correlation measurement device (CMD). The DDL is produced, by combining a mode \hat{b}_R , prepared in a strong and fully dephased coherent state, $\int_0^{2\pi} d\phi |\beta_R e^{i\phi}\rangle \langle \beta_R e^{i\phi}| / 2\pi$, $\beta_R \in \mathbb{R}$, with a comparatively weak local oscillator of complex amplitude β_D at a second beam splitter with amplitude transmittance T_D and reflectance R_D . In phase-space, the DDL has the form of a circle with the radius $|R_D|\beta_R$, which is required to be much greater than the absolute value of the complex displacement, $T_D\beta_D$, of the circle center. The DDL eliminates the coherent terms in the quadratures detected in balanced homodyne correlation measurements, see [22]. Its strong incoherent amplitude, β_R , guarantees a sufficiently strong field at the

CMD to record moments up to high orders. The signal displacement caused by the DDL, $\alpha = -RT_D\beta_D/T$, controls the position in phase-space, as desired in unbalanced homodyne detection. The signal \hat{a} undergoes the transformation

$$\hat{a}_0 = T(\hat{a} - \alpha) + RR_D\hat{b}_R, \quad (4)$$

which yields the field in the input channel of the CMD.

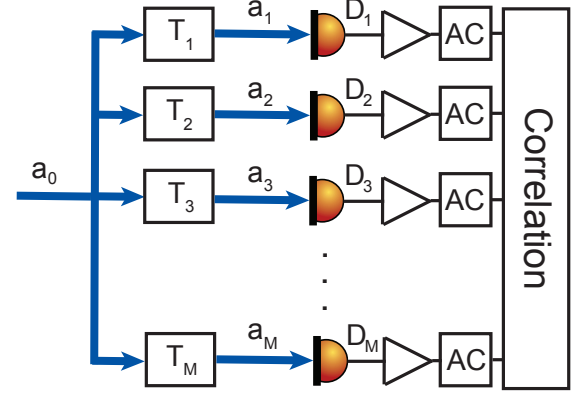


FIG. 2. (Color online) Structure of the CMD. The input mode is divided into M modes, each one being recorded by a detector. The amplitude in each channel is attenuated by an individual factor T_u , $u = 1, \dots, M$. The correlations in the AC parts of the amplified detector currents of different detectors are evaluated.

The structure of the CMD is shown in Fig. 2. The mode \hat{a}_0 is split into M output modes \hat{a}_u , $u = 1, \dots, M$. If T_u denotes the overall amplitude transmission through the path from mode \hat{a}_0 to mode \hat{a}_u , the simple relation

$$\hat{a}_u = T_u \hat{a}_0 + \text{vac} \quad (5)$$

holds true. The intensities of these modes are recorded by linear photodetectors with quantum efficiencies ζ_u . The electronic output signal of each detector is linearly amplified by a factor g_u , resulting in an electric current c_u . For our method to work properly, it is required that the mean currents (DC) \bar{c}_u are equal for all detectors, i.e., $g_u \zeta_u |T_u|^2 = \eta$, where η is an arbitrary but fixed positive constant. This is easily achieved by adjusting the individual gain factors g_u of the classical output currents of the detectors.

The measurement technique uses only the detected alternating currents (AC), labeled as \tilde{c}_u , to eliminate slow changes of the DDL parameters. The equal-time correlation of the AC sequences of $2m$ detectors,

$$\Gamma_{m,\alpha} = \overline{\tilde{c}_1 \cdots \tilde{c}_{2m}} = \binom{2m}{m} \tilde{\eta}^{2m} \langle : [\hat{n}(\alpha)]^m : \rangle, \quad (6)$$

with $\tilde{\eta} = \eta |T||R||R_D|\beta_R$, is proportional to the normal-ordered displaced number moment of power m . This expression follows from the photoelectric detection theory, cf., e.g., [25], together with Eqs. (4) and (5). In case of

amplitude fluctuations of the DDL, $\tilde{\eta}^{2m}$ is replaced with its statistical average, $\bar{\eta}^{2m}$. More details are given in Secs. C and G of the Appendix. Equation (6) is a central result of this contribution.

A strength of our technique compared to balanced homodyne detection is that no reference measurements like the vacuum detection for proper normalization is required, which would give rise to statistical uncertainties. Remarkably, even the dark noise appearing in each detector independently is erased by the UHCM technique. For a proof of this statement we refer to Sec. D of the Appendix. Furthermore, our method does not require photon-number resolving detectors. Even novel techniques, such as superconducting nanowire [26, 27] or transition-edge [28, 29] detectors, only resolve relatively small photon numbers. It is also important that our technique is insensitive to losses in the beam splitters, which naturally occur under experimental conditions. Moreover, it may be possible to implement the correlation of ACs by hardware, to obtain the moments $\langle : [\hat{n}(\alpha)]^m : \rangle$ very fast.

It is noteworthy that the generalization of our method to multimode radiation and even to space-time dependent correlation measurements is straightforward. In principle, one may use for each radiation mode a CMD of the type under study. The dephasing of the DDLs used for different modes must be statistically independent. The determination of space-time dependent quantum correlations of light [30] needs control of the relative time delays in the recorded data.

III. CERTIFICATION OF NONCLASSICALITY

A possible application of the UHCM technique is the certification of nonclassical properties of light. For this purpose it is convenient to consider observables of the form $\hat{W} = : \hat{f}^\dagger(\hat{a}, \hat{a}^\dagger) \hat{f}(\hat{a}, \hat{a}^\dagger) :.$ Whenever the measurement of such an observable yields a negative value, the state cannot be represented as a mixture of coherent states, $\hat{\rho} = \int d^2\alpha P_{\text{cl}}(\alpha) |\alpha\rangle\langle\alpha|$, with a classical probability distribution $P_{\text{cl}}(\alpha)$. Such states are referred to as nonclassical ones [31, 32].

Let us consider the operator

$$\hat{f}_{w,k}(\alpha) = \sum_{m=0}^k h_m w^{2m} [\hat{n}(\alpha)]^m, \quad (7)$$

with a positive constant w and the unit vector $\mathbf{h} = (h_0, \dots, h_k)^T$, which weights the powers of the displaced photon number operator. As we have seen above, our UHCM technique allows us to detect normal ordered moments of the displaced photon number. Hence, it can detect the function

$$F_{w,k}(\alpha) = \langle : \hat{f}_{w,k}^\dagger(\alpha) \hat{f}_{w,k}(\alpha) : \rangle = \mathbf{h}^T \underline{\mathbf{L}}(\alpha) \mathbf{h} \quad (8)$$

by determining the symmetric matrix of moments,

$$[\underline{\mathbf{L}}(\alpha)]_{mm'} = w^{2(m+m')} \langle : [\hat{n}(\alpha)]^{m+m'} : \rangle, \quad (9)$$

with $m, m' = 0, \dots, k$. The function (8) is completely determined, if the moments $\langle : [\hat{n}(\alpha)]^z : \rangle$ for $z = 1, \dots, 2k$ are known, which is feasible with exactly $4k$ detectors. If $F_{w,k}(\alpha) < 0$ for some α , then the state is nonclassical.

Interestingly, the function $F_{w,k}(\alpha)$ corresponds to the regularized quasiprobabilities $P_w(\alpha)$ in phase-space if one replaces in Eq. (8) $\mathbf{h} \mapsto \mathbf{H}$, where \mathbf{H} has the components

$$H_m = \frac{2^{1/q+1/2}}{\sqrt{\pi q} \Gamma(2/q)} \frac{(-1)^m}{(m!)^2} \Gamma\left(\frac{2}{q}(m+1)\right), \quad (10)$$

with $m = 0, \dots, \infty$, $\Gamma(\cdot)$ is the gamma function, and $q \in (2, \infty)$, for details see Sec. B of the Appendix. The function $P_w(\alpha)$ not only contains the full information about the quantum state of the signal field, it also provides a universal nonclassicality test [33, 34]. It approaches the Glauber-Sudarshan P function [35, 36] in the limit $w \rightarrow \infty$, see Ref. [33] and Sec. A of the Appendix. The regularized P function, P_w , was successfully reconstructed from quadrature data measured via balanced homodyne detection [37, 38]. This allows us also to verify nonclassical effects by negativities of this quasiprobability. However, such a reconstruction is quite sophisticated and requires the numerical calculation of pattern functions, cf. Supplement to [38]. Partial reconstruction of the regularized P function is feasible by applying in Eq. (8) for \mathbf{h} the $(k+1)$ -dimensional unit vector $\widetilde{\mathbf{H}}_k = \mathbf{H}_k / \|\mathbf{H}_k\|$, where the components of \mathbf{H}_k are equal to the first $(k+1)$ components of \mathbf{H} . The quantity

$$\mathcal{P}_{w,k}(\alpha) = \widetilde{\mathbf{H}}_k^T \underline{\mathbf{L}}(\alpha) \widetilde{\mathbf{H}}_k \quad (11)$$

is referred to as truncated regularized P function and is directly accessible via UHCM. In the case of an infinite number of detectors, a complete state reconstruction in terms of the regularized P function would be possible.

Note that the function $F_{w,k}(\alpha)$ contains only partial information for finite k . In general, the vector $\widetilde{\mathbf{H}}_k$ does not minimize the function $F_{w,k}(\alpha)$. To get an optimal nonclassicality test, we determine the minimal eigenvalue of the matrix (9),

$$\mathcal{F}_{w,k}(\alpha) = \min_{\mathbf{h}} F_{w,k}(\alpha) = \min \{S[\underline{\mathbf{L}}(\alpha)]\}, \quad (12)$$

where $S[\cdot]$ denotes the spectrum of a matrix. Hence, it holds that $\mathcal{F}_{w,k}(\alpha) \leq \mathcal{P}_{w,k}(\alpha)$ and also $\mathcal{F}_{w,k'}(\alpha) \leq \mathcal{F}_{w,k}(\alpha)$ for $k' > k$. Recently, a similar approach was proposed for multiple on-off detectors [39].

The matrix elements of $\underline{\mathbf{L}}(\alpha)$ are obtained from the measured correlation functions $\Gamma_{m,\alpha}$ in Eq. (6) as

$$[\underline{\mathbf{L}}(\alpha)]_{mm'} = \frac{\tilde{w}^{2(m+m')}}{\binom{2(m+m')}{m+m'}} \Gamma_{m+m',\alpha} \quad (13)$$

with the rescaled parameter $\tilde{w} = w/\tilde{\eta}$. The error calculation for $\mathcal{F}_{w,k}(\alpha)$ in (12) is somewhat involved and, hence, given in Sec. E of the Appendix. Our results show that the method yields nonclassicality tests with a high statistical significance. Of course, the statistical error can

be reduced by increasing the number of data points N , since the error is proportional to $N^{-1/2}$.

The above considerations are closely related to the matrix of moments approach of Agarwal and Tara [40]. Its generalization to displaced photon numbers, $[\underline{\mathbf{M}}(\alpha)]_{mm'} = \langle : [\hat{n}(\alpha)]^{m+m'} : \rangle$, yields, in the limit of infinite matrix dimension, the full information about nonclassicality. We want to stress that the existence of a negativity of $\mathcal{F}_{w,k}(\alpha)$ is independent of the value of w . Nevertheless, the statistical significance can be improved by properly adjusting this parameter. An advantage of our optimization is that exact values of the quantum efficiencies can be unknown to certify nonclassicality.

IV. RESULTS FOR SOME NONCLASSICAL STATES

The method described above is now applied to two different nonclassical states. The first one is a weakly squeezed vacuum state, $|\xi\rangle = \exp[(\xi^* \hat{a}^2 - \xi \hat{a}^{\dagger 2})/2]|\text{vac}\rangle$, with a relatively small value of $|\xi| = 0.03$. Therefore, it is very close to the vacuum state. The Wigner function of a squeezed vacuum state is known to be nonnegative and, thus, it does not certify nonclassicality by negative values.

Fig. 3 shows the truncated regularized P function for $k = 1, 2$ along the squeezed axis as well as the minimal eigenvalues $\mathcal{F}_{w,k}(\alpha)$. Both functions are multiplied with the same Gaussian function to suppress their polynomial divergence for increasing $|\alpha|$. This does not alter the sign of the functions. The function $\mathcal{F}_{w,1}(\alpha)$ is negative in a much larger α interval than $\mathcal{P}_{w,1}(\alpha)$. In the case of $k = 2$, the truncated regularized P function is nonnegative whereas the minimal eigenvalue is clearly negative for $|\text{Im}(\alpha)| \geq 0.13$. As k is increased, $\mathcal{P}_{w,k}(\alpha)$ approaches more and more the regularized P function. Remarkably, already $\mathcal{P}_{w,1}(\alpha)$ proves the nonclassicality very well. The negativities of $\mathcal{P}_{w,1}$ and $\mathcal{F}_{w,1}$ are for the same amount of data even more significant than those of $\mathcal{F}_{w,2}$, for details see Sec. F of the Appendix. This surprising result means that fewer detectors can even yield more insight than many detectors, also cf. similar conclusions for measurements with multiple on-off detectors [41].

As a second example, a single-photon-added thermal state (SPATS), $\hat{\rho} \propto \hat{a}^\dagger (\bar{n}/(1+\bar{n}))^{\bar{n}} \hat{a}$, is considered with the mean photon number \bar{n} of the thermal background. This state is comparable to a single photon state, which embodies the particle nature of light. For the overall quantum efficiency of $\eta = 0.5$ and $\bar{n} = 0.8$, several nonclassicality conditions have been tested [42], which could not certify quantumness. In Fig. 4 it is seen that the truncated regularized functions $\mathcal{P}_{w,k}$ are nonnegative for $w = 1.3$ and $k = 1, 2$. However, the minimal eigenvalue $\mathcal{F}_{w,k}$ attains negative values for $k \geq 2$, uncovering the nonclassical character of this state.

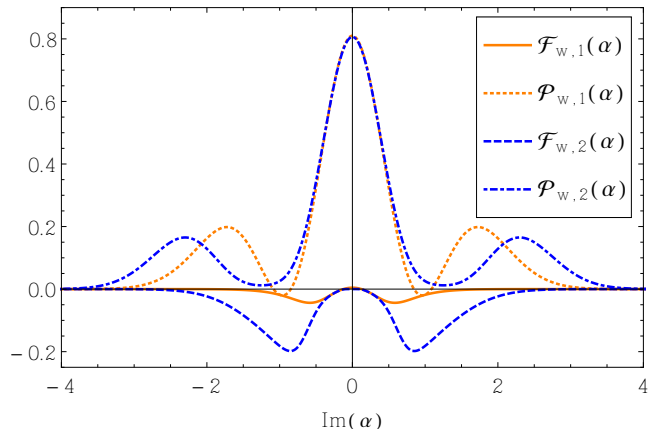


FIG. 3. (Color online) The minimal eigenvalues $\mathcal{F}_{w,k}(\alpha)$ and the truncated regularized P function $\mathcal{P}_{w,k}(\alpha)$ are shown for a squeezed vacuum state with $\xi = 0.03$ along the squeezed axis, for $q = 10$ and $w = 1.5$. All functions are multiplied with $\exp[-|\alpha|^2]$. The functions are illustrated for $k = 1$ and $k = 2$.

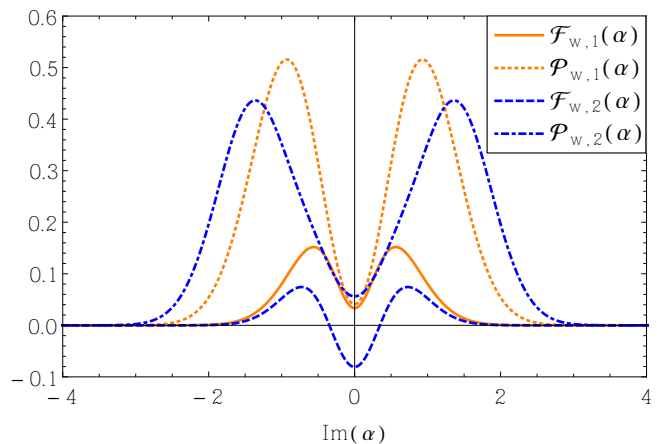


FIG. 4. (Color online) The minimal eigenvalues $\mathcal{F}_{w,k}(\alpha)$ and the truncated regularized P function $\mathcal{P}_{w,k}(\alpha)$ are shown for the SPATS with the parameters described in the text along the imaginary axis, for $q = 10$ and $w = 1.3$. All functions are multiplied with $\exp[-1.4|\alpha|^2]$. The functions are illustrated for $k = 1$ and $k = 2$.

V. CONCLUSIONS

In conclusion, we have proposed unbalanced homodyne correlation measurements for a direct experimental determination of normal-ordered displaced photon number moments, and, hence, for the quantum state representation in terms of these moments. This becomes feasible by interfering the signal field with a displaced dephased laser, recording the resulting light by a number of linear standard detectors, and correlating the alternating pho-

tocurrents. Photon number resolving detectors become superfluous.

phase-space.

ACKNOWLEDGMENTS

The determination of the minimal eigenvalue of the matrix of normal-ordered displaced number moments yields a powerful nonclassicality test with a high statistical significance. The test is directly accessible with our measurement technique. It is closely related to regularized quasiprobabilities visualizing nonclassicality in

This work was supported by the European Commission through the project QCUMbER (project reference: 665148) and by the Deutsche Forschungsgemeinschaft through SFB 652 (project B12). The authors gratefully acknowledge valuable comments by Jan Sperling and Boris Hage.

APPENDIX

Appendix A: Regularized P function

It is known, that the Glauber-Sudarshan P function is given by the Fourier transform of its characteristic function $\Phi(\beta)$, i.e.,

$$P(\alpha) = \frac{1}{\pi^2} \int d^2\beta \Phi(\beta) e^{\alpha\beta^* - \alpha^*\beta}. \quad (\text{A1})$$

Due to the fact, that the characteristic function $\Phi(\beta)$ for some states diverges for $|\beta| \rightarrow \infty$, the P function is in general highly singular, which prevents its experimental reconstruction. This problem is completely solved by so-called nonclassicality filters, $\Omega_w(\beta)$. These functions map $\Phi(\beta)$ to a new characteristic function $\Omega_w(\beta)\Phi(\beta)$, which corresponds to a regularized P function [33],

$$P_w(\alpha) = \frac{1}{\pi^2} \int d^2\beta \Omega_w(\beta) \Phi(\beta) e^{\alpha\beta^* - \alpha^*\beta}. \quad (\text{A2})$$

This phase-space distribution is a measurable counterpart of the P function and is also referred to as nonclassicality quasiprobability. The nonnegativity of the Fourier transform of the filter guarantees that negativities of P_w have its origin solely in the nonclassical character of the state and not in the filtering procedure. The regularized P function approaches the P function by increasing the filter width parameter, $w \rightarrow \infty$. Accordingly, a state is nonclassical, if there exists an $w < \infty$ and an α , so that $P_w(\alpha) < 0$. Our approach applies autocorrelation filters of the form

$$\Omega_w(\beta) = \frac{q2^{2/q-1}}{\pi\Gamma(2/q)w^2} \int d^2\beta' e^{-(|\beta'|/w)^q - (|\beta+\beta'|/w)^q}. \quad (\text{A3})$$

The parameter $q \in (2, \infty)$ fixes a particular filter function and $\Gamma(\cdot)$ is the gamma function.

Appendix B: Witnesses corresponding to regularized P functions

The regularized P function can be written as a convolution

$$P_w(\alpha) = \int d^2\gamma P(\gamma) \mathcal{F}[\Omega_w](\alpha - \gamma, \alpha^* - \gamma^*) \quad (\text{B1})$$

of the P function with the Fourier transform $\mathcal{F}[\cdot]$ of the nonclassicality filter,

$$\Omega_w(\beta) = \int d^2\beta' \tilde{f}_w^*(\beta', \beta'^*) \tilde{f}_w(\beta + \beta', \beta^* + \beta'^*). \quad (\text{B2})$$

The latter is an autocorrelation function of the function

$$\tilde{f}_w(\beta, \beta^*) = \frac{1}{w} \sqrt{\frac{q2^{2/q-1}}{\pi\Gamma(2/q)}} e^{-(|\beta|/w)^q}, \quad (\text{B3})$$

and, thus, its Fourier transform is given by

$$\mathcal{F}[\Omega_w](\alpha, \alpha^*) = \left| \mathcal{F}[\tilde{f}_w](\alpha, \alpha^*) \right|^2 = \langle \alpha | : \hat{f}_w^\dagger \hat{f}_w : | \alpha \rangle \quad (\text{B4})$$

with the definition

$$\hat{f}_w = \mathcal{F}[\tilde{f}_w](\hat{a}, \hat{a}^\dagger). \quad (\text{B5})$$

Applying relation (B4), the regularized P function (B1) can be rewritten as

$$\begin{aligned} P_w(\alpha) &= \int d^2\gamma P(\gamma) \langle \gamma | \hat{D}(\alpha) : \hat{f}_w^\dagger \hat{f}_w : \hat{D}^\dagger(\alpha) | \gamma \rangle \\ &= \langle \hat{W}(\alpha) \rangle, \end{aligned} \quad (\text{B6})$$

i.e., as the expectation value of a witness operator

$$\hat{W}(\alpha) = \hat{D}(\alpha) : \hat{f}_w^\dagger \hat{f}_w : \hat{D}^\dagger(\alpha). \quad (\text{B7})$$

In order to determine the operator function \hat{f}_w it is necessary to calculate the Fourier transform of (B3). One obtains for this quantity after a straightforward calculation

$$\mathcal{F}[\tilde{f}_w](\alpha, \alpha^*) = w \frac{2^{1/q+1/2}}{\sqrt{\pi q} \Gamma(2/q)} \sum_{m=0}^{\infty} \frac{(-w^2 |\alpha|^2)^m}{(m!)^2} \Gamma\left(\frac{2}{q}(m+1)\right), \quad (\text{B8})$$

and according to Eq. (B5)

$$\hat{f}_w = w \frac{2^{1/q+1/2}}{\sqrt{\pi q} \Gamma(2/q)} \sum_{m=0}^{\infty} \frac{(-1)^m}{(m!)^2} \Gamma\left(\frac{2}{q}(m+1)\right) w^{2m} \hat{n}^m. \quad (\text{B9})$$

With this last equation the witness operator (B7) is completely determined.

Appendix C: Equal-time correlation

In this section we relate the equal-time correlation

$$\Gamma_{m,\alpha} = \overline{\tilde{c}_1 \cdots \tilde{c}_{2m}}, \quad (\text{C1})$$

of the alternating currents (AC), \tilde{c}_u , of $2m$ different detectors of the UHCM setup in Figs. 1 and 2 of the main text, to the moment $\langle : [\hat{n}(\alpha)]^m : \rangle$. In the further calculation the AC \tilde{c}_u is assumed to be obtained by subtracting the mean current \bar{c}_u (DC) from the photocurrent c_u . The expression (C1) can be related to quantum mechanical expectation values by using photoelectric detection theory [25],

$$\begin{aligned} \Gamma_{m,\alpha} &= \overline{(c_1 - \bar{c}_1) \cdots (c_{2m} - \bar{c}_{2m})} \\ &= (g_1 \cdots g_{2m}) (\zeta_1 \cdots \zeta_{2m}) \left\langle : [\hat{a}_1^\dagger \hat{a}_1 - \langle \hat{a}_1^\dagger \hat{a}_1 \rangle] \cdots [\hat{a}_{2m}^\dagger \hat{a}_{2m} - \langle \hat{a}_{2m}^\dagger \hat{a}_{2m} \rangle] : \right\rangle. \end{aligned} \quad (\text{C2})$$

Here ζ_u and g_u are the quantum efficiency of the detector D_u and the gain factor of the output current, respectively. Using the relation

$$\hat{a}_u = T_u \hat{a}_0 + \text{vac}, \quad (\text{C3})$$

between the modes \hat{a}_0 and \hat{a}_u , the latter recorded by detector D_u , Eq. (C2) can be rewritten as

$$\Gamma_{m,\alpha} = \eta^{2m} \left\langle : \left[\hat{a}_0^\dagger \hat{a}_0 - \langle \hat{a}_0^\dagger \hat{a}_0 \rangle \right]^{2m} : \right\rangle, \quad (\text{C4})$$

where the balance condition $g_u \zeta_u |T_u|^2 = \eta$, for all $u = 1, \dots, 2m$, is used. This is easily done by adjusting the g_u values of the amplifiers. The signal \hat{a} is combined with the field of a displaced dephased laser (DDL) at a highly transmitting beam splitter with amplitude transmittance T and reflectance R . The DDL is produced by combining the field \hat{b}_R of a fully dephased coherent state of amplitude $\beta_R \in \mathbb{R}$ with a coherent state of amplitude β_D at a beam splitter with amplitude transmittance T_D and reflectance R_D . In total this can be described by the relation

$$\hat{a}_0 = T(\hat{a} - \alpha) + RR_D \hat{b}_R, \quad (\text{C5})$$

with $\alpha = -RT_D\beta_D/T$. The corresponding number operator reads as

$$\hat{n}_0 = |T|^2\hat{n}(\alpha) + |R|^2|R_D|^2\hat{b}_R^\dagger\hat{b}_R + T^*RR_D(\hat{a}^\dagger - \alpha^*)\hat{b}_R + TR^*R_D^*(\hat{a} - \alpha)\hat{b}_R^\dagger, \quad (\text{C6})$$

where $\hat{n}(\alpha)$ is the displaced photon number operator $\hat{n}(\alpha) = (\hat{a}^\dagger - \alpha^*)(\hat{a} - \alpha)$. Since the mode \hat{b}_R is in the dephased coherent state, $\int_0^{2\pi} d\phi |\beta_R e^{i\phi}\rangle \langle \beta_R e^{i\phi}| / (2\pi)$, one gets for the expectation value of \hat{n}_0 the expression

$$\langle \hat{n}_0 \rangle = |T|^2 \langle \hat{n}(\alpha) \rangle + |R|^2 |R_D|^2 \beta_R^2. \quad (\text{C7})$$

Inserting these results into Eq. (C4), one may derive

$$\Gamma_{m,\alpha} = \frac{(\eta|T|)^{2m}}{2\pi} \int_0^{2\pi} d\phi \left\langle : [|T|(\hat{n}(\alpha) - \langle \hat{n}(\alpha) \rangle) + |R||R_D|(\hat{a}^\dagger - \alpha^*)\beta_R e^{i\phi} + |R||R_D|(\hat{a} - \alpha)\beta_R e^{-i\phi}]^{2m} : \right\rangle. \quad (\text{C8})$$

In the limit of a strong amplitude β_R , this expression simplifies to

$$\begin{aligned} \Gamma_{m,\alpha} &= (\eta|T||R||R_D|\beta_R)^{2m} \frac{1}{2\pi} \int_0^{2\pi} d\phi \left\langle : [(\hat{a}^\dagger - \alpha^*)e^{i\phi} + (\hat{a} - \alpha)e^{-i\phi}]^{2m} : \right\rangle \\ &= (\eta|T||R||R_D|\beta_R)^{2m} \binom{2m}{m} \langle : [\hat{n}(\alpha)]^m : \rangle. \end{aligned} \quad (\text{C9})$$

Introducing the new variable $\tilde{\eta} = \eta|T||R||R_D|\beta_R$, one arrives at the final result

$$\Gamma_{m,\alpha} = \binom{2m}{m} \tilde{\eta}^{2m} \langle : [\hat{n}(\alpha)]^m : \rangle. \quad (\text{C10})$$

Appendix D: Irrelevance of dark noise in UHCM

The joint-event statistics, for recording m_1 photons at detector D_1 , m_2 photons at detector D_2 and so on, with including dark noise $\hat{\nu}_u$ of detector D_u , is given by

$$P_{m_1, \dots, m_M} = \left\langle : \frac{(\eta_1 \hat{n}_1 + \hat{\nu}_1)^{m_1}}{m_1!} e^{-(\eta_1 \hat{n}_1 + \hat{\nu}_1)} \dots \frac{(\eta_M \hat{n}_M + \hat{\nu}_M)^{m_M}}{m_M!} e^{-(\eta_M \hat{n}_M + \hat{\nu}_M)} : \right\rangle. \quad (\text{D1})$$

In an analogous manner as in Eq. (C2) we derive

$$\begin{aligned} \Gamma_{m,\alpha} &= \overline{(c_1 - \bar{c}_1) \cdots (c_{2m} - \bar{c}_{2m})} \\ &= (g_1 \cdots g_{2m}) \left\langle : \prod_{u=1}^{2m} [\zeta_u (\hat{n}_u - \langle \hat{n}_u \rangle) + (\hat{\nu}_u - \langle \hat{\nu}_u \rangle)] : \right\rangle. \end{aligned} \quad (\text{D2})$$

The dark counts in different detectors are assumed to be uncorrelated, but may obey arbitrary statistics. Therefore, one obtains

$$\Gamma_{m,\alpha} = (g_1 \cdots g_{2m}) (\zeta_1 \cdots \zeta_{2m}) \langle : (\hat{n}_1 - \langle \hat{n}_1 \rangle) \cdots (\hat{n}_{2m} - \langle \hat{n}_{2m} \rangle) : \rangle. \quad (\text{D3})$$

Obviously, this result is the same as Eq. (C2), where the dark noise is ignored.

Appendix E: Error calculation

This section outlines the determination of the error bar for the minimal eigenvalue of the $(k+1) \times (k+1)$ matrix of moments,

$$[\mathbf{L}(\alpha)]_{mm'} = \mathcal{M}_{m+m',\alpha}, \quad (\text{E1})$$

where

$$\mathcal{M}_{\ell,\alpha} = w^{2\ell} \langle : [\hat{n}(\alpha)]^\ell : \rangle. \quad (\text{E2})$$

For this purpose, in a first step the error of the elements of this matrix is calculated in a straight forward manner. The measurement of $\langle : [\hat{n}(\alpha)]^m : \rangle$ requires $2m$ different detectors. Accordingly, to obtain the matrix (E1) the number

M of detectors has to be greater than or equal to $4k$. As derived in Section C, the equal-time correlation of $2m$ ACs yields the elements of the matrix (E1), i.e.,

$$\mathcal{M}_{\ell,\alpha} = \frac{\tilde{w}^{2\ell}}{\binom{2\ell}{\ell}} \overline{\tilde{c}_1 \cdots \tilde{c}_{2\ell}}. \quad (\text{E3})$$

with $\tilde{w} = w/\tilde{\eta}$. Let N be the number of data samples used to calculate this correlation. Then the sampling error of $\mathcal{M}_{\ell,\alpha}$ is calculated as

$$\Delta \mathcal{M}_{\ell,\alpha} = \frac{\tilde{w}^{2\ell}}{\sqrt{N} \binom{2\ell}{\ell}} \sqrt{\overline{\tilde{c}_1^2 \cdots \tilde{c}_{2\ell}^2} - (\overline{\tilde{c}_1 \cdots \tilde{c}_{2\ell}})^2}. \quad (\text{E4})$$

The first expectation value on the right hand side can be evaluated as

$$\begin{aligned} \overline{\tilde{c}_1^2 \cdots \tilde{c}_{2\ell}^2} &= \overline{(c_1 - \bar{c}_1)^2 \cdots (c_{2\ell} - \bar{c}_{2\ell})^2} \\ &= \sum_{v_1=0}^{\infty} \cdots \sum_{v_{2\ell}=0}^{\infty} P_{v_1, \dots, v_{2\ell}} (g_1[v_1 - \bar{v}_1])^2 \cdots (g_{2\ell}[v_{2\ell} - \bar{v}_{2\ell}])^2, \end{aligned} \quad (\text{E5})$$

where the joint-event statistics,

$$P_{v_1, \dots, v_{2\ell}} = \left\langle : \frac{(\zeta_1 \hat{n}_1)^{v_1}}{v_1!} e^{-\zeta_1 \hat{n}_1} \cdots \frac{(\zeta_{2\ell} \hat{n}_{2\ell})^{v_{2\ell}}}{v_{2\ell}!} e^{-\zeta_{2\ell} \hat{n}_{2\ell}} : \right\rangle, \quad (\text{E6})$$

is the probability to measure v_1 photocounts at detector D_1 , v_2 photocounts at detector D_2 , and so on. It is easy to show by using photoelectric detection theory [25], the balance condition $g_u \zeta_u |T_u|^2 = \eta$, and relation (C3), that (E5) simplifies to

$$\begin{aligned} \overline{\tilde{c}_1^2 \cdots \tilde{c}_{2\ell}^2} &= (g_1 \zeta_1)^2 \cdots (g_{2\ell} \zeta_{2\ell})^2 \left\langle : \prod_{u=1}^{2\ell} [(\hat{n}_u - \langle \hat{n}_u \rangle)^2 + \hat{n}_u / \zeta_u] : \right\rangle \\ &= \eta^{4\ell} \left\langle : \prod_{u=1}^{2\ell} [(\hat{n}_0 - \langle \hat{n}_0 \rangle)^2 + \hat{n}_0 / (\zeta_u |T_u|^2)] : \right\rangle. \end{aligned} \quad (\text{E7})$$

For the subsequent calculation, it is advantageous to introduce additionally the symbol

$$\Xi_{\ell,p} = \sum_{\substack{\mathcal{U} \subseteq \{1, \dots, 2\ell\} \\ |\mathcal{U}| = 2\ell - p}} \prod_{u \in \mathcal{U}} \frac{1}{\zeta_u |T_u|^2}, \quad p = 0, \dots, 2\ell. \quad (\text{E8})$$

Now, the further evaluation of (E7) yields

$$\overline{\tilde{c}_1^2 \cdots \tilde{c}_{2\ell}^2} = \eta^{4\ell} \sum_{p=0}^{2\ell} \Xi_{\ell,p} \left\langle : (\hat{n}_0 - \langle \hat{n}_0 \rangle)^{2p} \hat{n}_0^{2\ell - p} : \right\rangle. \quad (\text{E9})$$

The quantum mechanical expectation values can be related to the signal field by considering the combination (C5) of the signal field \hat{a} with the displaced dephased laser at a beam splitter as

$$\begin{aligned} \overline{\tilde{c}_1^2 \cdots \tilde{c}_{2\ell}^2} &= \eta^{4\ell} \sum_{p=0}^{2\ell} \Xi_{\ell,p} \frac{1}{2\pi} \int_0^{2\pi} d\phi \\ &\quad \times \left\langle : [|T|^2 (\hat{n}(\alpha) - \langle \hat{n}(\alpha) \rangle) + |T||R||R_D|(\hat{a}^\dagger - \alpha^*)\beta_R e^{i\phi} + |T||R||R_D|(\hat{a} - \alpha)\beta_R e^{-i\phi}]^{2p} \right. \\ &\quad \times [|T|^2 \hat{n}(\alpha) + |R|^2 |R_D|^2 \beta_R^2 + |T||R||R_D|(\hat{a}^\dagger - \alpha^*)\beta_R e^{i\phi} + |T||R||R_D|(\hat{a} - \alpha)\beta_R e^{-i\phi}]^{2\ell - p} : \left. \right\rangle \\ &= \eta^{4\ell} \sum_{p=0}^{2\ell} \Xi_{\ell,p} \sum_{a_1 + a_2 + a_3 = 2p} \binom{2p}{a_1, a_2, a_3} \sum_{b_1 + b_2 + b_3 = 2\ell - p} \binom{2\ell - p}{b_1, b_2, b_3} \\ &\quad \times |T|^{2a_1} (-|T|^2 \langle \hat{n}(\alpha) \rangle)^{a_2} (|T||R||R_D|\beta_R)^{a_3} |T|^{2b_1} (|R|^2 |R_D|^2 \beta_R^2)^{b_2} (|T||R||R_D|\beta_R)^{b_3} \\ &\quad \times 1[(a_3 + b_3) \text{ even}] \binom{a_3 + b_3}{(a_3 + b_3)/2} \left\langle : [\hat{n}(\alpha)]^{a_1 + b_1 + (a_3 + b_3)/2} : \right\rangle. \end{aligned} \quad (\text{E10})$$

Here $1[a]$ is 1 if a is true, and 0 otherwise. Inserting Eq. (E2) and Eq. (E10) into Eq. (E4), yields the error $\Delta\mathcal{M}_{\ell,\alpha}$. This expression is useful to determine the error without the need for simulating experimental data. For the recorded ACs $\{\tilde{c}_u^{(t)}\}_{t=1}^N$ of $2m$ different detectors D_u , each sequence containing N data samples, the sampling error may be determined by the formula

$$\Delta\mathcal{M}_{\ell,\alpha} = \sqrt{\frac{1}{N(N-1)} \sum_{t=1}^N \left[\frac{\tilde{w}^{2\ell}}{\binom{2\ell}{\ell}} \tilde{c}_1^{(t)} \cdots \tilde{c}_{2\ell}^{(t)} - \mathcal{M}_{\ell,\alpha} \right]^2}. \quad (\text{E11})$$

Using the error $[\Delta\mathbf{L}(\alpha)]_{mm'} = \Delta\mathcal{M}_{m+m',\alpha}$ of the elements of the matrix $\mathbf{L}(\alpha)$, the error of the minimal eigenvalue,

$$\mathcal{F}_{w,k}(\alpha) = \min \{S[\mathbf{L}(\alpha)]\}, \quad (\text{E12})$$

of this matrix with the spectrum S , is obtained by performing a linear error propagation. If the unit vector $\mathbf{v} \equiv \mathbf{v}_{w,k}(\alpha)$ is an eigenvector corresponding to the minimal eigenvalue (E12), the error of $\mathcal{F}_{w,k}(\alpha)$ reads as

$$\Delta\mathcal{F}_{w,k}(\alpha) = |\mathbf{v}|^T \Delta\mathbf{L}(\alpha) |\mathbf{v}|, \quad (\text{E13})$$

where $|\mathbf{v}| = (|v_0|, \dots, |v_k|)$. From Eqs. (E12) and (E13) one may determine the statistical significance as

$$\Sigma = \begin{cases} |\mathcal{F}_{w,k}(\alpha)| / \Delta\mathcal{F}_{w,k}(\alpha) & \text{if } \mathcal{F}_{w,k}(\alpha) < 0 \\ 0 & \text{else} \end{cases}. \quad (\text{E14})$$

Appendix F: Statistical Significance

In the main text a weakly squeezed vacuum state and a single-photon-added thermal state are considered. Figs. 5 and 6 show the statistical significances Σ of the negativities of $\mathcal{F}_{w,k}(\alpha)$ and $\mathcal{P}_{w,k}(\alpha)$ for these states. The significance is determined according to Eq. (E14). In Fig. 1 the value of Σ is zero for $\mathcal{P}_{w,2}(\alpha)$ and in Fig. 2 the only nonvanishing Σ -value occurs for $\mathcal{F}_{w,2}(\alpha)$. A significance of $\Sigma \gtrsim 5$ clearly certifies the nonclassicality of the state.

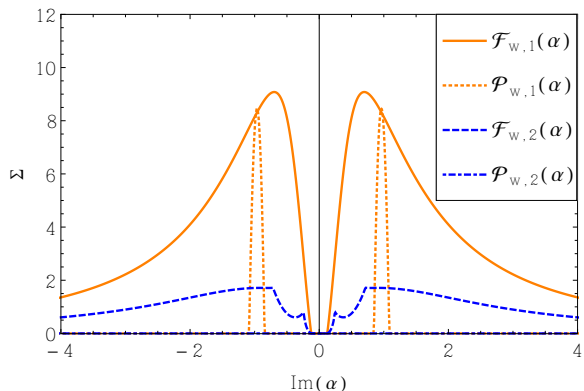


FIG. 5. (Color online) The statistical significance Σ for $N = 10^6$ data samples is shown for the minimal eigenvalues $\mathcal{F}_{w,k}(\alpha)$ and the truncated regularized P function $\mathcal{P}_{w,k}(\alpha)$ for a squeezed vacuum state with $\xi = 0.03$ along the squeezed axis, for $q = 10$ and $w = 1.5$. The functions are illustrated for $k = 1$ and $k = 2$.

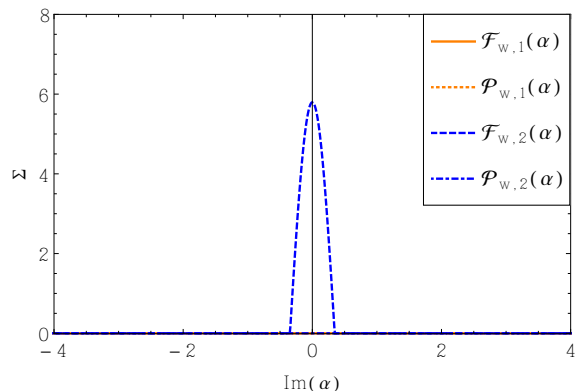


FIG. 6. (Color online) The statistical significance Σ for $N = 10^7$ data samples is shown for the minimal eigenvalues $\mathcal{F}_{w,k}(\alpha)$ and the truncated regularized P function $\mathcal{P}_{w,k}(\alpha)$ for the SPATS with the parameters described in the main text along the imaginary axis, for $q = 10$ and $w = 1.3$. The functions are illustrated for $k = 1$ and $k = 2$.

Appendix G: Amplitude fluctuations of the DDL

Since we are dealing with unbalanced homodyne measurements, we must consider amplitude fluctuation effects of the DDL. In this case we replace Eq. (6) in the main text with

$$\Gamma_{m,\alpha} = \overline{\tilde{c}_1 \cdots \tilde{c}_{2m}} = \binom{2m}{m} \overline{\tilde{\eta}^{2m}} \langle : [\hat{n}(\alpha)]^m : \rangle, \quad (\text{G1})$$

$$\overline{\tilde{\eta}^{2m}} = (\eta|T||R||R_D|)^{2m} \overline{\beta_R^{2m}}. \quad (\text{G2})$$

Let us assume that the amplitude fluctuations, $\Delta\beta_R = \beta_R - \overline{\beta_R}$, are Gaussian. In typical experiments, the relative intensity fluctuations can be stabilized to about 10^{-2} , over time intervals of the order needed for state reconstruction. For moments of increasing order the effects of amplitude noise are increasing. The examples in the main text require moments of fourth order, for which we consider the noise effects. For Gaussian noise the leading terms are

$$\overline{\beta_R^4} \approx \overline{\beta_R}^4 \left(1 + 28 \frac{\overline{\Delta\beta_R^2}}{\overline{\beta_R}^2} \right) \approx \overline{\beta_R}^4 (1 + 7 \times 10^{-4}). \quad (\text{G3})$$

Hence for moments up to fourth order it is still a very good approximation to ignore the amplitude fluctuations. In case of higher-order moments the amplitude fluctuations can be recorded in an auxiliary channel in Fig. 1, and the measured correlations according to Eq. (G1) can be corrected by dividing with the recorded $\overline{\beta_R^{2m}}$ values. The relative intensity fluctuations of the DDL are further reduced by correcting the data within sufficiently small time intervals.

-
- [1] J. H. Shapiro, H. P. Yuen, and J. A. Machado Mata, *Optical Communication with Two-Photon Coherent States – Part II: Photoemissive Detection and Structured Receiver Performance*, IEEE Trans. Inf. Theory **25**, 179 (1979).
 - [2] H. P. Yuen and V. W. S. Chan, *Noise in homodyne and heterodyne detection*, Opt. Lett. **8**, 177 (1983).
 - [3] G. L. Abbas, V. W. S. Chan, and T. K. Yee, *Local-oscillator excess-noise suppression for homodyne and heterodyne detection*, Opt. Lett. **8**, 419 (1983).
 - [4] D. T. Smithey, M. Beck, M. G. Raymer, and A. Faridani, *Measurement of the Wigner distribution and the density matrix of a light mode using optical homodyne tomography: Application to squeezed states and the vacuum*, Phys. Rev. Lett. **70**, 1244 (1993).
 - [5] Serge Haroche, *Nobel Lecture: Controlling photons in a box and exploring the quantum to classical boundary*, Rev. Mod. Phys. **85**, 1083 (2013).
 - [6] David J. Wineland, *Nobel Lecture: Superposition, entanglement, and raising Schrödinger’s cat*, Rev. Mod. Phys. **85**, 1103 (2013).
 - [7] E. Bimbard, R. Boddeda, N. Vitrant, A. Grankin, V. Parigi, J. Stanojevic, A. Ourjoumtsev, and P. Grangier, *Homodyne Tomography of a Single Photon Retrieved on Demand from a Cavity-Enhanced Cold Atom Memory*, Phys. Rev. Lett. **112**, 033601 (2014).
 - [8] D.-G. Welsch, W. Vogel, and T. Opatrný, *Homodyne detection and quantum-state reconstruction*, Prog. Opt. **39**, 63 (1999).
 - [9] U. Leonhardt, *Measuring the Quantum State of Light* (Cambridge University Press, Cambridge, 2005).
 - [10] A. I. Lvovsky and M. G. Raymer, *Continuous-variable optical quantum-state tomography*, Rev. Mod. Phys. **81**, 299 (2009).
 - [11] A. Royer, *Measurement of the Wigner Function*, Phys. Rev. Lett. **55**, 2745 (1985).
 - [12] S. Wallentowitz and W. Vogel, *Unbalanced homodyning for quantum state measurements*, Phys. Rev. A **53**, 4528 (1996).
 - [13] K. Banaszek, C. Radzewicz, K. Wódkiewicz, *Direct measurement of the Wigner function by photon counting*, Phys. Rev. A **60**, 674 (1999).
 - [14] H. J. Kimble, M. Dagenais, and L. Mandel, *Photon Antibunching in Resonance Fluorescence*, Phys. Rev. Lett. **39**, 691 (1977).
 - [15] L. Mandel, *Squeezed States and Sub-Poissonian Photon Statistics*, Phys. Rev. Lett. **49**, 136 (1982).
 - [16] W. Vogel, *Squeezing and anomalous moments in resonance fluorescence*, Phys. Rev. Lett. **67**, 2450 (1991).
 - [17] W. Vogel, *Homodyne correlation measurements with weak local oscillators*, Phys. Rev. A **51**, 4160 (1995).
 - [18] C. H. H. Schulte, J. Hansom, A. E. Jones, C. Matthiesen, C. Le Gall, M. Atatüre, *Quadrature squeezed photons from a two-level system*, Nature **525**, 222 (2015).
 - [19] H. J. Carmichael, H. M. Castro-Beltran, G. T. Foster, and L. A. Orozco, *Giant Violations of Classical Inequalities through Conditional Homodyne Detection of the Quadrature Amplitudes of Light*, Phys. Rev. Lett. **85**, 1855 (2000).
 - [20] G. T. Foster, L. A. Orozco, H. M. Castro-Beltran, and H. J. Carmichael, *Quantum State Reduction and Conditional Time Evolution of Wave-Particle Correlations in Cavity QED*, Phys. Rev. Lett. **85**, 3149 (2000).
 - [21] S. Gerber, D. Rotter, L. Slodička, J. Eschner, H. J. Carmichael, and R. Blatt, *Intensity-Field Correlation of*

- Single-Atom Resonance Fluorescence*, Phys. Rev. Lett. **102**, 183601 (2009).
- [22] E. Shchukin and W. Vogel, *Universal Measurement of Quantum Correlations of Radiation*, Phys. Rev. Lett. **96**, 200403 (2006).
- [23] K. E. Cahill and R. J. Glauber, *Ordered Expansions in Boson Amplitude Operators*, Phys. Rev. **177**, 1857 (1969).
- [24] T. Kiesel and W. Vogel, *Complete nonclassicality test with a photon-number-resolving detector*, Phys. Rev. A **86**, 032119 (2012).
- [25] W. Vogel and D.-G. Welsch, *Quantum Optics*, 3rd ed. (Wiley-VCH, Weinheim, 2006).
- [26] A. Divochiy et al., *Superconducting nanowire photon-number resolving detector at telecommunication wavelengths*, Nature Photonics **2**, 302 (2008).
- [27] S. Jahanmirinejad et al., *Photon-number resolving detector based on a series array of superconducting nanowires*, Appl. Phys. Lett. **101**, 072602 (2012).
- [28] D. H. Smith et al., *Conclusive quantum steering with superconducting transition-edge sensors*, Nature Communications **3**, 625 (2012).
- [29] B. Calkins et al., *High quantum-efficiency photon-number-resolving detector for photonic on-chip information processing*, Opt. Express **21**, 22657 (2013).
- [30] W. Vogel, *Nonclassical Correlation Properties of Radiation Fields*, Phys. Rev. Lett. **100**, 013605 (2008).
- [31] U. M. Titulaer and R. J. Glauber, *Correlation Functions for Coherent Fields*, Phys. Rev. **140**, B676 (1965).
- [32] L. Mandel, *Non-Classical States of the Electromagnetic Field*, Phys. Scr. **T12**, 34 (1986).
- [33] T. Kiesel and W. Vogel, *Nonclassicality filters and quasiprobabilities*, Phys. Rev. A **82**, 032107 (2010).
- [34] B. Kühn and W. Vogel, *Visualizing nonclassical effects in phase space*, Phys. Rev. A **90**, 033821 (2014).
- [35] R. J. Glauber, *Coherent and Incoherent States of the Radiation Field*, Phys. Rev. **131**, 2766 (1963).
- [36] E. C. G. Sudarshan, *Equivalence of Semiclassical and Quantum Mechanical Descriptions of Statistical Light Beams*, Phys. Rev. Lett. **10**, 277 (1963).
- [37] T. Kiesel, W. Vogel, M. Bellini, and A. Zavatta, *Nonclassicality quasiprobability of single-photon-added thermal states*, Phys. Rev. A **83**, 032116 (2011).
- [38] T. Kiesel, W. Vogel, B. Hage, and R. Schnabel, *Direct Sampling of Negative Quasiprobabilities of a Squeezed State*, Phys. Rev. Lett. **107**, 113604 (2011).
- [39] J. Sperling, M. Bohmann, W. Vogel, G. Harder, B. Brecht, V. Ansari, and C. Silberhorn, *Uncovering Quantum Correlations with Time-Multiplexed Click Detection*, Phys. Rev. Lett. **115**, 023601 (2015).
- [40] G. S. Agarwal and K. Tara, *Nonclassical character of states exhibiting no squeezing or sub-Poissonian statistics*, Phys. Rev. A **46**, 485 (1992).
- [41] A. Luis, J. Sperling, and W. Vogel, *Nonclassicality Phase-Space Functions: More Insight with Fewer Detectors*, Phys. Rev. Lett. **114**, 103602 (2015).
- [42] A. Zavatta, V. Parigi, and M. Bellini, *Experimental nonclassicality of single-photon-added thermal light states*, Phys. Rev. A **75**, 052106 (2007).